Formation of Isolated Nickel-Centered Gallium Clusters in $Na_{10}Ga_{10}Ni$ and a 2-D Network of Gallium Octahedra in K_2Ga_3

Robert W. Henning and John D. Corbett*

Department of Chemistry and Ames Laboratory—DOE,[1] Iowa State University, Ames, Iowa 50011

Received March 25, 1999

Exploration of the sodium−gallium−nickel system has revealed a new compound containing the isolated gallium clusters $Ga_{10}Ni^{10-}$. Single-crystal X-ray diffraction studies of $Na_{10}Ga_{10}Ni$ (*Pnma*, $Z = 12$, $a = 13.908(3)$ Å, $b = 28.146(6)$ Å, $c = 16.286(4)$ Å) show it to be isostructural with $K_{10}In_{10}Ni$. The compound contains two similar "naked" gallium clusters as distorted, tetracapped trigonal prismatic units that are centered by nickel. The sodium atoms serve to isolate the clusters from each other as well as to provide the cluster with a closed shell configuration of electrons. This is the first isolated gallium cluster in an alkali-metal system that is centered. Molecular orbital calculations on the cluster are also reported. The crystal structure of K_2Ga_3 (*I*4/*mmm*, $Z = 4$, $a = 6.1382(3)$ Å, $c = 14.815(1)$ Å) has also been established to be isostructural with A_2In_3 (A = Rb, Cs). This contains Ga_6^{4-} octahedra interconnected through the waist atoms into layers $^2_\infty[Ga_6^{4-}]$, with octahedra in adjacent layers sitting in the depressions of the first. The potassium atoms have characteristic roles except for an unusually short K−K contact (3.242(4) Å) across the layer. Magnetic measurements indicate that both phases are diamagnetic and consistent with the Zintl formalism.

Introduction

The alkali-metal−gallium systems are well-known for the formation of numerous cluster network compounds.[2] Many of the clusters are related to the deltahedral clusters found in borane chemistry, such as Ga_6 and Ga_{12}, but others such as Ga_{15} and Ga_{17} have unique geometries. As in borohydride chemistry, the skeletal electron counts in the individual deltahedral clusters usually follow Wade's rules[3] when electron transfer from the cations is included, meaning the compounds are electron precise and are Zintl phases.[4] For classical closo-deltahedra, *n*-atom clusters require $2n + 2$ electrons for skeletal bonding, assuming an additional formal s pair is left on each vertex atom. Since the members of the gallium family do not form sufficiently stable exo bonds to hydrogen, alkyl, etc., a fairly large negative charge (oxidation state) of $-n - 2$ is necessary for isolated closo clusters. Only Ga_6^{8-} is known in the presence of higher field cations in $Ba_5Ga_6H_2$.[5] Although these classical species do not appear to be favorable for gallium, *closo*-Tl_5^{7-} [6] and *nido*-In_4^{8-} and -Tl_4^{8-},[7] among others, are known for its heavier congeners.

Alternatively, such clusters may reduce their charge by oxidation and the formation of exo bonds (links) to other clusters or to gallium spacers between clusters to give network structures. These are commonly observed for gallium,[2] e.g., in AGa_3 (A = Rb,[8] Cs[9]) and in $Na_{22}Ga_{39}$.[10] A new process, the distortion of clusters away from the ideal deltahedral symmetries, has also been found to reduce the number of skeletal electrons needed and give stability. This has been observed with the heavier triels (Tr = Ga, In, Tl) in the hypoelectronic $(2n - 2)$ Tr_{11}^{7-} for A_8Tr_{11} (A = K, Rb, some Cs)[4] and $A_8Tr_{11}X$ (X = Cl, Br, I).[11] Another way found to reduce the cluster charge is the introduction of an interstitial atom, as in the thallium-centered icosahedral Tl_{13}^{11-} in $Na_3K_8Tl_{13}$.[12] Both centering and cluster distortion are needed to stabilize the related $K_8Tr_{10}Zn$ (for In[13] and Tl[14]) and $K_{10}In_{10}Ni$,[15] which is isostructural with the present $Na_{10}Ga_{10}Ni$. Since the alkali-metal−gallium systems are much better known for cluster network formation, the discovery of the discrete cluster $Ga_{10}Ni^{10-}$ is quite novel.

The formation of K_2Ga_3, another Zintl phase, is an example of condensation in which gallium octahedra form two-dimensional layers. This structure type is already known for A_2In_3 (A = Rb, Cs).[16] The existence of the composition K_2Ga_3 was established earlier,[2,17] but no structural assignment was possible.

Experimental Section

Handling of all reactants and products took place in gloveboxes filled with N_2 or He (≤0.1 ppm of H_2O per volume) because of the general sensitivity of these materials to air and moisture. Amounts of the

(1) This research was supported by the Office of the Basic Energy Sciences, Materials Sciences Division, U.S. Department of Energy. Ames Laboratory is operated by Iowa State University under Contract No. W-7405-Eng.82.

(2) Belin, C.; Tillard-Charbonnel, M. *Prog. Solid State Chem.* **1993**, *22*, 59.
(3) Wade, K. Adv. *Inorg. Chem. Radiochem.* **1976**, *18*, 1.
(4) Corbett, J. D. *Struct. Bonding* **1997**, *87*, 157.
(5) Henning, R. W.; Leon-Escamilla, E. A.; Zhao, J.-T.; Corbett, J. D. *Inorg. Chem.* **1997**, *36*, 1282.
(6) Dong, Z.-C.; Corbett, J. D. *J. Am. Chem. Soc.* **1994**, *116*, 3429.
(7) Sevov, S. C.; Corbett, J. D. *J. Solid State Chem.* **1993**, *103*, 114.
(8) Ling, R. G.; Belin, C. *Z. Anorg Allg. Chem.* **1981**, *480*, 181.
(9) van Vucht, J. H. N. *J. Less-Common Met.* **1985**, *108*, 163.
(10) Ling, R. G.; Belin, C. *Acta Crystallogr.* **1982**, *B38*, 1101.
(11) Henning, R. W.; Corbett, J. D. *Inorg. Chem.* **1997**, *36*, 6045.
(12) Dong, Z. C.; Corbett, J. D. *J. Am. Chem. Soc.* **1995**, *117*, 6447.
(13) Sevov, S. C.; Corbett, J. D. *Inorg. Chem.* **1993**, *32*, 1059.
(14) Dong, Z. C.; Henning, R. W.; Corbett, J. D. *Inorg. Chem.* **1997**, *36*, 3559.
(15) Sevov, S. C.; Corbett, J. D. *J. Am. Chem. Soc.* **1993**, *115*, 9089.
(16) Sevov, S. C.; Corbett, J. D. *Z. Anorg. Allg. Chem.* **1993**, *619*, 128.
(17) Tillard-Charbonnel, M.; Chouzibi, N.; Belin, C. *C. R. Acad. Sci., Ser. II* **1990**, *311*, 69.

10.1021/ic990335l CCC: $18.00
Published on Web 07/30/1999

elements sufficient to gain the stoichiometric title compounds were welded into tantalum tubing using techniques described previously.[12] Potassium (99.95%, Alfa), gallium (99.99%, Johnson-Matthey), and nickel (99.99%, Johnson-Matthey, 100 mesh) were used as received while the surface of the sodium metal (99.9%, Alfa) was cleaned with a scalpel before use. The reaction mixtures were heated to 650 °C, held there for 24 h to ensure homogeneity of the samples, and then slowly cooled (3 °C/h) to room temperature.

$Na_{10}Ga_{10}Ni$. The dull gray, microcrystalline product formed at this composition was ~100% $Na_{10}Ga_{10}Ni$ according to a comparison Guinier powder pattern calculated after the structural study was finished. Potentially suitable crystals were sealed into thin-walled capillaries and checked for singularity by Laue photographs. Diffraction data were collected on a Rigaku AFC6R rotating-anode diffractometer at room temperature with the aid of Mo Kα radiation. An orthorhombic unit cell was determined from 25 reflections collected by random search. Two octants of data ($h,\pm k,l$) were measured up to 50° in 2θ and corrected for Lorentz and polarization effects. Of the 14 801 reflections measured, 6902 were observed ($I \geq 3\sigma_I$) and 2684 of these were unique. Three ψ scans were used to correct the data for absorption ($\mu = 135.2$ cm^{-1}). Systematic absences and the intensity distribution gave a strong indication that the structure had the centrosymmetric space group *Pnma* (No. 62).

Application of direct methods[18] revealed 19 heavy-atom positions, two of which were assigned to nickel on the basis of interatomic distances, and the remainder, to gallium. Refinement of their positional parameters followed by a difference Fourier synthesis revealed all 17 peaks appropriate for sodium. Isotropic refinement of all atoms ($R(F) = 10.2\%$) followed by DIFABS[19] reduced $R(F)$ to 9.6%. The last step provided nearly spherical ellipsoids and smaller standard deviations for all parameters. Anisotropic refinement of all atoms then converged at $R(F)$, $R_w = 6.2$, 6.3%. With 298 variables, the reflection:variable ratio was small, ~9:1. More data at higher angles would presumably have improved the refinement, but the combination of a weakly diffracting crystal with a large unit cell made such data collection unreasonable with the point-source techniques then available. A question arose as to whether the sodium atoms should only be refined isotropically, which would reduce the number of variables to 204 and increase the corresponding reflection: parameter ratio to ~13:1. However, such a refinement did not change $R(F)$ or any other factors appreciably. Although Hamilton's test[20] suggested that refinement of anisotropic thermal parameters for the sodium was not statistically meaningful, their full refinement is still reported. The largest positive and negative peaks in the final difference Fourier map were 2.91 e/Å^3 (1.85 Å from Ga6A) and −1.77 e/Å^3. All refinements were carried out on a VAX workstation using the TEXSAN crystallographic package.[21]

K_2Ga_3. This product also was obtained in high yield, but it is more sensitive to moisture and air than are most compounds in the alkali-metal−gallium systems. This made sharp Guinier powder patterns difficult to obtain in the usual way using cellophane tape for mounting. The crystals had a metallic luster and were very brittle. Single crystals were handled and data collection was performed as above. Twenty-five reflections obtained from a random search were indexed on a body-centered tetragonal unit cell. Four octants of reflection data ($h,\pm k,\pm l$) were then collected at room temperature with Mo Kα radiation up to 60° in 2θ and corrected as above. No violation of the body-centering was observed. Absorption was corrected with the aid of six ψ-scans collected over a range of 2θ angles. Systematic absences and the N(Z) distribution suggested the unique centrosymmetric space group *I*4/*mmm* (No. 139), and this allowed a successful refinement. Four other space groups possible for the observed absences, *I*422, *I*4*mm*, $I\bar{4}2m$, and $I\bar{4}m2$, are all noncentrosymmetric.

The structure solution obtained by direct methods[18] contained four peaks, two of which were assigned to gallium and two of which were assigned to potassium on the basis of interatomic distances. The refinement proceeded smoothly to $R(F) = R_w = 1.8\%$ at convergence. The largest positive and negative peaks in the final difference map were 1.26 e/Å^3 (1.74 Å from K1) and −0.45 e/Å^3. Some data collection parameters and the atom positions plus isotropic-equivalent thermal parameters for the two structures are given in Tables 1−3, while distances in K_2Ga_3 are listed in Table 4. Additional data collection and refinement parameters and anisotropic thermal parameters for both structures are given in the Supporting Information together with distances in $Na_{10}Ga_{10}Ni$ (because of their extent). These and the F_o/F_c data are also available from J.D.C.

Property Measurements. Magnetic susceptibility measurements were collected with the aid of a Quantum Design MPMS SQUID

Table 1. Data Collection and Refinement Parameters for $Na_{10}Ga_{10}Ni$ and K_2Ga_3

	$Na_{10}Ga_{10}Ni$	K_2Ga_3
crystal size (mm)	0.27 × 0.23 × 0.22	0.09 × 0.12 × 0.25
space group, Z	*Pnma* (No. 62), 12	*I*4/*mmm* (No. l39), 4
lattice parameters[a]		
a (Å)	13.908(3)	6.1382(3)
b (Å)	28.146(6)	
c (Å)	16.286(4)	14.815(1)
V (Å^3)	6375(4)	558.17(7)
d_{calc} (g/cm^3)	3.081	3.419
μ(Mo Kα) (cm^{-1})	134.76	156.67
$R_{av}(I \geq 3\sigma_I)$ (%)	5.6	2.7
residuals R, R_w[b] (%)	6.2, 6.3	1.8, 1.8

[a] Guinier data with Si as an internal standard; $\lambda = 1.540\,562$ Å; 23 °C. [b] $R = \sum||F_o| - |F_c||/\sum|F_o|$; $R_w = [\sum w(|F_o| - |F_c|)^2/\sum w(F_o)^2]^{1/2}$, $w = 1/\sigma_F^2$.

Table 2. Positional and Thermal Parameters for $Na_{10}Ga_{10}Ni$

atom	Wyckoff posn	x	y	z	B_{eq} (Å^2)[a]
Ga1A	8*d*	0.8644(2)	0.4257(1)	0.9737(2)	2.0(1)
Ga2A	8*d*	0.8690(2)	0.4764(1)	0.1256(2)	1.9(1)
Ga3A	8*d*	0.7236(2)	0.4934(1)	0.0097(2)	1.8(1)
Ga4A	8*d*	0.7574(2)	0.3367(1)	0.0247(2)	2.1(1)
Ga5A	8*d*	0.7701(2)	0.4093(1)	0.2344(2)	1.9(1)
Ga6A	8*d*	0.5692(2)	0.4270(1)	0.0776(2)	1.9(1)
Ga7A	8*d*	0.8935(2)	0.3725(1)	0.1216(2)	2.6(1)
Ga8A	8*d*	0.6740(2)	0.4830(1)	0.1712(2)	1.8(1)
Ga9A	8*d*	0.6707(2)	0.4067(1)	0.9459(2)	1.8(1)
Ga10A	8*d*	0.6510(2)	0.3538(1)	0.1572(2)	2.4(1)
NiA	8*d*	0.7448(2)	0.4167(1)	0.0855(2)	0.9(1)
Ga1B	8*d*	0.8440(2)	0.6970(1)	0.1481(2)	2.2(1)
Ga2B	4*c*	0.8673(3)	3/4	−0.0034(3)	2.3(2)
Ga3B	8*d*	0.6441(2)	0.6780(1)	0.1482(2)	2.2(1)
Ga4B	4*c*	0.6405(3)	3/4	0.9483(2)	2.5(2)
Ga5B	4*c*	0.7229(4)	3/4	0.2392(2)	2.5(2)
Ga6B	8*d*	0.7397(2)	0.6768(1)	0.0041(2)	2.1(1)
Ga7B	4*c*	0.5420(3)	3/4	0.0974(2)	1.9(2)
NiB	4*c*	0.7183(3)	3/4	0.0854(3)	1.3(2)
Na1	8*d*	0.6669(8)	0.5845(3)	0.9217(6)	2.9(5)
Na2	4*c*	0.691(1)	1/4	−0.085(1)	3.6(8)
Na3	8*d*	0.5054(8)	0.3353(4)	0.0044(6)	3.0(5)
Na4	8*d*	0.9254(8)	0.5431(4)	0.9651(7)	4.1(6)
Na5	8*d*	0.8095(9)	0.3506(4)	0.8282(7)	3.7(6)
Na6	8*d*	0.5672(9)	0.3433(5)	0.8049(7)	4.7(7)
Na7	8*d*	0.5110(8)	0.4250(4)	0.2554(6)	3.6(6)
Na8	8*d*	0.0082(8)	0.3420(4)	0.9680(7)	3.7(6)
Na9	4*c*	0.522(1)	3/4	0.302(1)	5(1)
Na10	8*d*	0.766(1)	0.5860(4)	0.1249(6)	3.9(6)
Na11	8*d*	0.710(1)	0.4851(4)	0.8177(6)	4.1(6)
Na12	8*d*	0.523(1)	0.5404(6)	0.0833(7)	6.4(8)
Na13	8*d*	0.537(1)	0.5433(5)	0.3160(7)	5.0(7)
Na14	8*d*	0.868(1)	0.6756(5)	0.8438(7)	5.3(7)
Na15	4*c*	0.895(1)	1/4	0.078(1)	6(1)
Na16	4*c*	0.634(2)	1/4	0.121(1)	5(1)
Na17	8*d*	0.607(1)	0.6808(4)	0.7982(8)	6.8(9)

[a] $B_{eq} = (8\pi^2/3)\sum_i\sum_j U_{ij}a_i^*a_j^*\vec{a}_i\vec{a}_j$.

(18) Sheldrick, G. M. SHELXS-86. Universität Göttingen, Germany, 1986.
(19) Walker, N.; Stuart, D. *Acta Crystallogr.* **1983**, *A39*, 158.
(20) Stout, G. H.; Jensen, L. H. *X-ray Structure Determination*; Wiley: New York, 1989; p 388.
(21) *TEXSAN*, version 6.0; Molecular Structure Corp.: The Woodlands, TX, 1990.

Table 3. Positional and Thermal Parameters for K_2Ga_3

atom	Wyckoff posn	*x*	*y*	*z*	B_{eq} (Å^2)[a]
Ga1	4*e*	0	0	0.13886(6)	1.43(2)
Ga2	8*i*	0.2947(1)	0	0	1.20(2)
K1	4*e*	0	0	0.3906(1)	2.55(5)
K2	4*d*	0	1/2	1/4	2.33(5)

[a] $B_{eq} = (8\pi^2/3)\sum_i\sum_j U_{ij} a_i^* a_j^* \vec{a}_i \vec{a}_j$.

Table 4. Bond Distances in K_2Ga_3 ($d < 5$ Å)

Ga1−Ga2	×4	2.7393(8)	K1−K1		3.242(4)
Ga1−K1		3.729(2)	K1−K2	×4	3.709(1)
Ga1−K2	×4	3.4829(4)	K1−Ga1		3.729(2)
Ga2−Ga2		2.521(1)	K1−Ga2	×8	3.6927(9)
Ga2−Ga2	×2	2.5579(8)	K2−K1	×4	3.709(1)
Ga2−Ga1	×2	2.7393(8)	K2−K2	×4	4.3404(2)
Ga2−K1	×4	3.6927(9)	K2−Ga2	×4	3.9123(3)
Ga2−K2	×2	3.9123(3)	K2−Ga1	×4	3.4829(4)

magnetometer. The air sensitivity of $Na_{10}Ga_{10}Ni$ and K_2Ga_3 required the use of a special sample holder. This was built from a 3 mm i.d. silica tube ~7 cm long and two silica rods, 3 mm in diameter and ~8 cm long, that fit snugly inside the larger tube. One rod was fused into the bottom of the tube. Powdered $Na_{10}Ga_{10}Ni$ (29.2 mg) or K_2Ga_3 (50.3 mg) was then placed inside the tube in a He-filled glovebox, and the second rod was inserted to hold the sample between the two rods. The latter was then fused to the outer tube to seal the container. The susceptibility of each sample was measured in a field of 3 T over the temperature range 6−300 K. The raw data sets were each corrected for the sample holder and diamagnetism of the cores, the latter amounting to -1.42×10^{-4} and -5.0×10^{-5} emu/mol for $Na_{10}Ga_{10}Ni$ and K_2Ga_3, respectively.

Bonding Calculations. Molecular orbital calculations were performed on the $Ga_{10}Ni^{10-}$ cluster using the EHMACC program on a PC. The H_{ii} parameters used were −14.58 and −6.75 eV for Ga 4s and 4p[22] and −9.17, −5.15, and −13.49 eV for Ni 4s, 4p, and 3d,[23] respectively.

Results and Discussion

$Na_{10}Ga_{10}Ni$. The most interesting structural features of $Na_{10}Ga_{10}Ni$ are the two independent 10-atom gallium clusters each centered by nickel, $Ga_{10}Ni^{10-}$. The gallium atoms in both can be viewed (Figure 1) as strongly distorted trigonal prisms with all three rectangular faces and one trigonal face capped by gallium. The pseudo-3-fold axes in these lie vertical. The trigonal face (dashed lines) that is capped at the top by Ga6 or Ga7 is expanded so that all Ga−Ni contacts are nearly equidistant (2.459(6)−2.529(4) Å, Supporting Information). These are consistent with the Ga−Ni contacts in Ni_2Ga_3, which range over 2.38−2.61 Å and average 2.50 Å for eight distances.[24] The Ga−Ga distances in the clusters are typical for those with delocalized (electron-deficient) bonding of this sort (2.6−2.9 Å). Clusters A and B are present in a 2:1 ratio and have similar geometries (~C_{3v}) except that B lies on a mirror plane containing Ni, Ga2, Ga4, Ga5, and Ga7 while A is in a general position. Even though the basic geometries of the two clusters are the same, comparison of Ga−Ga distances shows that some of these vary between clusters by as much as ~0.11 Å, with more consistent bond lengths in the asymmetric unit. Each unit cell contains 12 clusters, with the closest Ga−Ga contact between them at 4.88 Å (Figure 2). The thermal parameters for the two nickel atoms are slightly smaller than those for gallium, consistent with the usual behavior of other

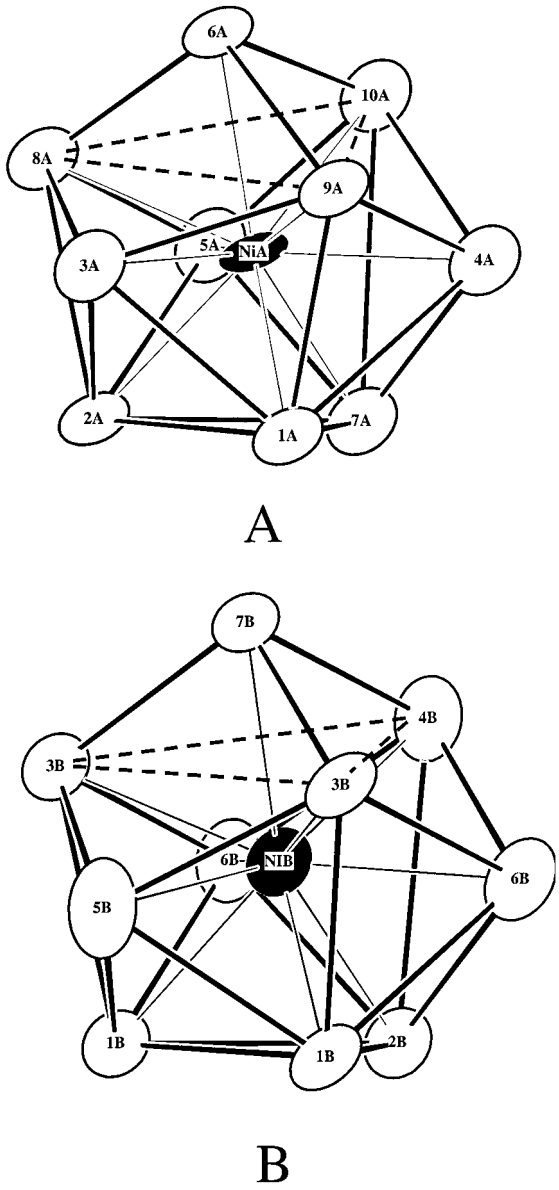

Figure 1. The two independent cluster anions A and B in $Na_{10}Ga_{10}Ni$ (80% probability ellipsoids).

clusters with a more tightly bound central atom. The gallium atoms have relatively low coordination numbers in these clusters and fairly weak bonding to the cations, so they exhibit larger but close to spherical thermal ellipsoids. Their definition is also limited by the size of the data set obtained (Experimental Section).

The clusters are arranged in close-packed layers parallel to the *b*−*c* plane with hexagonal stacking of the layers along the *a* axis (Figure 3). Since the clusters are roughly spherical, the close-packing leaves large trigonal antiprismatic voids between the layers. Many of these cavities are appropriately sized for the sodium cations, with Na−Ga and Na−Na contacts in the ranges of 3.0−3.3 and 3.35−3.6 Å, respectively. Some of the interlayer holes are also a little larger (radius ≥~3.2 Å), and the cations therein are more poorly bound, with only two or three contacts in the above range. In all but one case (Na12), the latter correspond to those with $B_{eq} \geq 5$ Å^2. Additional sodium atoms lie between clusters within the layers, and these appear more tightly bound to gallium with smaller ellipsoids (~3.5 Å^2; Figure 2). Attempts to substitute potassium into this structure always resulted in the formation of K_2Ga_3.

(22) Canadell, E.; Eisenstein, O.; Rubio, J. *Organometallics* **1984**, *3*, 759.
(23) Lauher, J. W.; Elian, M.; Summerville, R. H.; Hoffmann, R. *J. Am. Chem. Soc.* **1976**, *98*, 3219.
(24) Hellner, E.; Laves, F. *Z. Naturforsch.* **1947**, *2A*, 177.

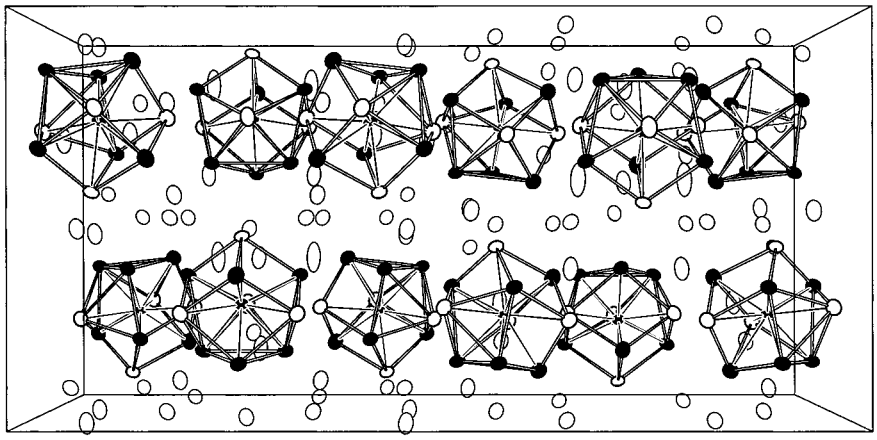

Figure 2. [001] view of the unit cell of $Na_{10}Ga_{10}Ni$ showing its layered nature. The atoms defining the distorted trigonal prisms are black, and the capping atoms are white. The B clusters lie on mirror planes at $y = {}^1/_4, {}^3/_4$ (50% ellipsoids).

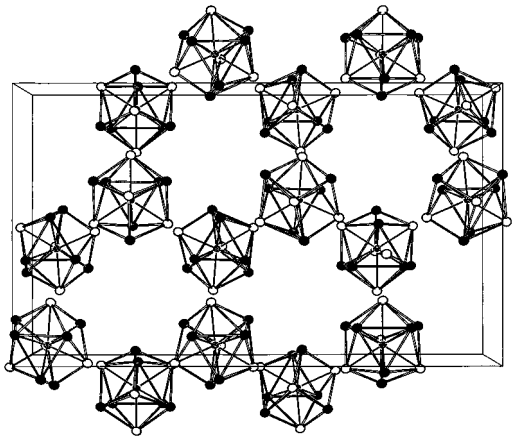

Figure 3. A [100] view of the $Na_{10}Ga_{10}Ni$ structure showing the pseudohexagonal-close-packed nature of the cluster disposition and the large cavities between in which some of the cations are bound (50%). Black atoms define the (distorted) trigonal prisms.

The geometry of $Ga_{10}Ni^{10-}$ is unusual in its low symmetry relative to, for example, Ga_{11}^{7-} (a pentacapped trigonal prism) and the isoelectronic $In_{10}Zn^{8-}$ (a centered square antiprism). One major difference, and a likely explanation for the contrast in the shape of the present clusters, is the increased number of cations to be accommodated. This is of particular importance because alkali-metal cations in all triel cluster and network structures are always observed to exhibit some combination of face capping, edge bridging, or exo bonding to the vertexes on the clusters. As discussed in more detail for $In_{10}Ni$,[10−15] the relatively larger number of cations here evidently leads to distortion of the polyhedron so as to generate more edges and faces and, at the same time, a more open structure because of the additional cation−cation repulsions. This change also leads to more and somewhat longer Tr−Tr bonds at each vertex.

Although $Na_{10}Ga_{10}Ni$ can be prepared in ∼100% yield by slow cooling of the melt, it is difficult to obtain single crystals large enough for single-crystal X-ray diffraction. Extended equilibrations (over 1 month) at various temperatures resulted in decomposition of $Na_{10}Ga_{10}Ni$ into $Na_{22}Ga_{39}$, Ni_2Ga_3, and a small amount of sodium. Also, reactions that had been loaded off-stoichiometry either produced one of the known binaries or, in the case of sodium, left that element. Lattice constants from Guinier powder patterns of reactions loaded off-stoichiometry indicated that $Na_{10}Ga_{10}Ni$ is a line compound within 3σ. Attempts to incorporate the heavier palladium and platinum atoms into the clusters failed, in contrast to the cases of the $K_{10}In_{10}Z$ and $K_{10}Tl_{10}Z$[25] analogues. Reactions with earlier transition metals (Co, Cr, Fe) likewise failed, presumably because of their lower electron counts as far as this product is concerned (below).

The heavier analogue $K_{10}In_{10}Ni$[15] showed similar problems, with large thermal ellipsoids for certain cations, but in general it appeared to be more stable than $Na_{10}Ga_{10}Ni$, giving a well-crystallized phase without any sign of side products. Several factors may affect the relative stability of these two phases. While other phases in alkali-metal−gallium systems containing isolated clusters are presently only Cs_8Ga_{11}, $Cs_8Ga_{11}X$, and $Rb_8Ga_{11}X$ (X = Cl, Br, I),[11] indium is more productive of isolated clusters, and thallium gives an abundance of these. Perhaps this trend arises from an increasing stability of what are substantially s^2 lone pairs on each cluster vertex as one moves from Ga to Tl and the clear opposite trend, the formation of stronger 2c−2e intercluster bonds, in the other direction (Tl → Ga). The second trend is related to the first as cluster condensation, which is most prevalent with gallium,[2] can be viewed as a result of a one-electron oxidation of the s^2 pairs at each vertex in the process. Another factor affecting the relative stability of $K_{10}In_{10}Ni$ is the lack of comparable decomposition products; Ni_2In_3 is known but the analogous $K_{22}In_{39}$ is not.

(a) Bonding. EHMO calculations were performed on the isolated $Ga_{10}Ni^{10-}$ cluster as well as on the analogous unit without a nickel atom to gain a better understanding of the bonding. All calculations were performed on a slightly modified cluster with true C_{3v} symmetry since the observed deviations therefrom split pseudodegenerate energy levels by only about 0.06 eV.

The lowest 10 orbitals for the empty cluster between −10 and −20 eV (Figure 4) represent principally linear combinations of the lone $4s^2$ pairs at each gallium vertex, only the highest one near −10 eV showing some mixing with Ga 4p. On the other hand, the 10 bonding orbitals just below the HOMO−LUMO gap (dashed, ∼−6.0 eV) are formed primarily from Ga 4p orbitals in the empty cage. Incorporation of nickel into the cluster does not have a significant effect on most of the molecular orbitals of the empty cage. Some mixing of the five relatively contracted Ni 3d orbitals into the corresponding gallium cluster orbitals around −14 eV lowers these ∼1 eV, but five higher energy nickel orbital combinations are also added since all are filled in such a well-reduced system. Most of the effective bonding between the centering atom and the cluster occurs via Ni 4s and Ga 4p, principally with p_z orbitals in the

(25) Z.-C. Dong and J. D. Corbett, unpublished research.

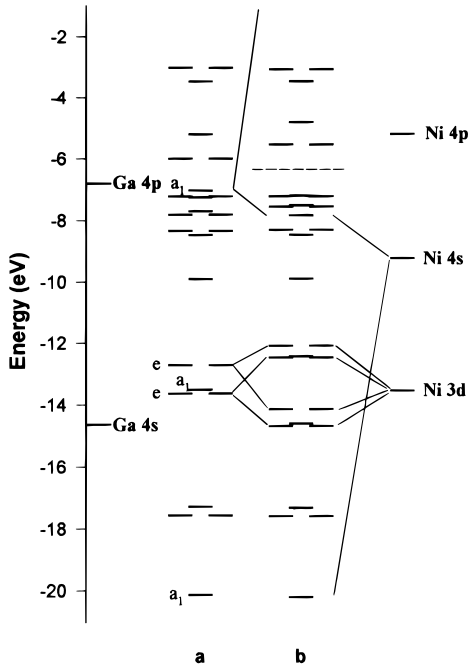

Figure 4. Molecular orbital diagrams for the empty Ga_{10} unit (a) and the $Ga_{10}Ni^{10-}$ cluster (b). The evident Fermi energy is dashed.

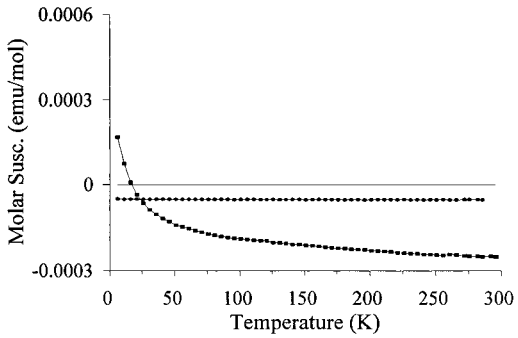

Figure 5. Magnetic susceptibilities of $Na_{10}Ga_{10}Ni$ (lower, filled squares) and K_2Ga_3 (filled circles) at 3 T as a function of temperature (K).

a_1 cage orbital near −7 eV. The latter is lowered ∼1 eV while the antibonding combination is pushed much higher (∼10 eV). The net result is that d^{10} nickel does not introduce any new bonding orbitals but does stabilize a few cluster orbitals through Ni 4s−Ga 4p bonding. The Ni 4p orbitals are higher and do not contribute significantly.

(b) Properties. Magnetic susceptibilities obtained for $Na_{10}Ga_{10}Ni$ (Figure 5) indicate that it is diamagnetic, consistent with the closed-shell nature predicted for it. The temperature dependence at the lower end may be intrinsic. However, although the Guinier powder pattern indicated the sample was single phase (≥∼96%), a small amount of a ferromagnetic impurity could still be present, especially considering the metastable nature of $Na_{10}Ga_{10}Ni$. A similar trend in the data was observed for $K_{10}In_{10}Ni$.[15]

K_2Ga_3. The main building blocks in tetragonal K_2Ga_3 are gallium octahedra that are interconnected via the Ga2 waist atoms into a layered compound, leaving Ga1 atoms as the apexes (Figure 6). The clusters have local D_{4h} symmetry while the extended net is a 4^4-layer of octahedra. The octahedra of adjacent layers also sit in the depressions of the first, creating a body-centered unit cell. This rather rare structure type has been observed only for Cs_2In_3 and Rb_2In_3,[16] so it is not surprising to find it in the gallium system with an appropriately smaller cation.

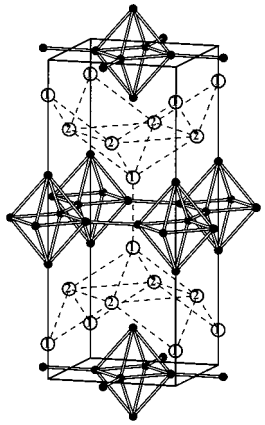

Figure 6. Body-centered tetragonal unit cell of K_2Ga_3 showing the $^2_\infty[Ga_6^{4-}]$ layers (filled circles) normal to $\bar{c}$ and the interlayer K^+ positions (open circles, numbered by type). The dashed lines between cations indicate the similarity of their packing to that of the anionic net structure in $NaGa_4$ ($BaAl_4$ type).[26]

The Ga−Ga bond distances within each cluster (Table 4) are consistent with those in the related Rb_2In_3 phase. The apical Ga1 forms four equivalent bonds to Ga2 at 2.7393(8) Å. Each five-bonded Ga2 atom is connected to two Ga1 apex atoms, to two more Ga2 waist atoms at a shorter 2.5579(8) Å, and exo to a Ga2 in an adjacent cluster at a still shorter 2.521(1) Å.

The potassium functionality is fairly regular and can be understood by reference to Figure 6. (The dashed lines pertain to a relationship of their pattern to the network in $NaGa_4$, below.) Each K1 lies on a 4-fold axis at $^1/_2$, z and as such caps Ga2−Ga1−Ga2 faces on four interlinked octahedra in a fairly uniform way. Each K1 atom also lies exo to a Ga1 vertex in another layer at a similar distance. The related K2 atoms that form a square array on the cell faces each bridge Ga1−Ga2 edges on two pair of adjoining octahedra related by a $\bar{4}$ axis. These bridging K2 atoms are 0.43 Å closer to Ga1 vertexes than to the Ga2 waist atoms, but the average d(K2−Ga) distance is close to the more symmetric d(K1−Ga) distance. The crowding of the cations in this phase, in contrast to that in the isostructural Rb_2In_3, is particularly seen in the short K1−K1 separation of 3.242(4) Å through the square holes in the cluster layers (center of Figure 6). The 0.24 Å decrease of the A1−A1 distance from that in Rb_2In_3 because of the triel lattice contraction is only 55% of the average reduction in other $d(A^+-A^+)$. The tetragonal elongation of each cluster probably arises because of cation repulsions and their "fit" with the cluster layers. The Ga1-(apex)−K2 distances are notably short.

The electronic description of K_2Ga_3 in a classical sense is fairly easy. In terms of Wade's rules, an isolated octahedron requires $2n + 2 = 14$ skeletal electrons, viz., Ga_6^{8-} with inert "s pairs" remaining at each vertex. Oxidation by four electrons at the waist to afford the layer bonding would give Ga_6^{4-}, or $(K^+)_4Ga_6^{4-}$. This makes K_2Ga_3 a closed-shell compound and a Zintl phase, an assignment consistent with the diamagnetism of this phase shown in Figure 5. The net diamagnetism, -5.0×10^{-5} emu·mol^{-1}, is very similar to that of the poor semiconductor Rb_2In_3.

A closer look at the cation arrangement in K_2Ga_3 reveals a framework that is quite similar to that of the gallium atoms in the approximately antitypic $NaGa_4$ ($BaAl_4$ type).[26] Gallium in

(26) Bruzzone, G. *Acta Crystallogr.* **1969**, *25B*, 1206.

the latter phase generates a layer of edge-sharing square pyramids with adjacent apexes pointing in opposite directions. The apex of each pyramid is also bonded with a like atom in the adjacent layer. This is the same pattern that the potassium atoms exhibit in K_2Ga_3 (dashed lines). The sodium atoms in $NaGa_4$ sit in the large holes generated by the interbonded gallium layers, substituting for the cluster units in the present phase.

Conclusions

Binary alkali-metal−gallium systems are well-known for their formation of network structures containing exo-bonded deltahedral gallium clusters, the high formal charge on the hypothetical cluster parents being alleviated by the cluster interbonding. The present K_2Ga_3 is a good and still simple example of this type of connectivity. The only exceptions to this simple trend occur with Cs_8Ga_{11} and related halide compounds, which contain isolated Ga_{11}^{7-} units, and the ideal Ga_6^{8-} in $Ba_5Ga_6H_2$.[5] Ternary gallium phases with the late transition metals also produce framework materials but with other, often complex, structure types, typically with mixed occupancy of the anionic sites, e.g., $Na_{35}Cd_{24}Ga_{56}$[27] and $Na_{128}Au_{81}Ga_{275}$.[28] This strong tendency to form extended structures makes the formation of isolated $Ga_{10}Ni^{10-}$ units in $Na_{10}Ga_{10}Ni$ an even more interesting result. Moreover, this compound also conforms to the modified Zintl concepts that have been well established in this area of the periodic table.

Acknowledgment. We are grateful to J. Ostenson for the magnetic susceptibility measurements.

Supporting Information Available: Tables of additional crystallographic information and anisotropic thermal parameters for both compounds and a listing of distances in $Na_{10}Ga_{10}Ni$. This material is available free of charge via the Internet at http://pubs.acs.org.

IC990335L

(27) Tillard-Charbonnel, M.; Belin, C. *Mater. Res. Bull.* **1992**, *27*, 1277.
(28) Tillard-Charbonnel, M.; Belin, C. *Z. Kristallogr.* **1993**, *206*, 310.